


Concurrent Progression of Through and Turning Movements for Arterials Experiencing Heavy Turning Flows and Bay-Length Constraints

Yen-Hsiang Chen¹, Yao Cheng¹, and Gang-Len Chang¹

Transportation Research Record
2019, Vol. 2673(9) 525–537
© National Academy of Sciences:
Transportation Research Board 2019
Article reuse guidelines:
sagepub.com/journals-permissions
DOI: 10.1177/0361198119843480
journals.sagepub.com/home/trr


Abstract

Contending with congestion on major urban arterials by providing progression bands has long been a priority task for the traffic community. However, on an arterial experiencing heavy left-turn volumes at major intersections, the left-turn queue may spill back rapidly and further degrade the effectiveness of the through progression band if the left-turn volume and the limited bay length have not been accounted for in the optimization of signal coordination plan. Such negative impact from left-turn queues also justifies the need to take into account the concurrent progression of through and left-turn flows on major arterials. To address these two issues, this paper presents a three-staged signal optimization model that can circumvent or minimize the impact of left-turn spillback to the through movements and concurrently minimize the delay of left-turn flows. The proposed model firstly obtains an initial maximized bandwidth from an existing state-of-the-art method and then maximizes the portion of through bandwidth not impeded by the left-turn overflows. The delay of left-turn flows at each intersection will also be minimized under the obtained effective through bandwidth. The results from the numerical analyses have confirmed the benefits and need of including the left-turn volume and its bay length in the design of dual progression for through and left-turn movements. The simulation experiments further show a reduction in the average delay and the number of stops, by 6.4% and 5.5%, respectively, for vehicles traversing an arterial segment of six intersections, compared with the state-of-the-art model, MULTIBAND.

Contending with congestion on major urban arterials has long been a priority task for traffic professionals. Over the past several decades, most studies focusing on this subject have been conducted along the two distinct lines of delay minimization and signal progression optimization. In the former category, TRANSYT, a simulation-based optimization model, is one of the most adopted tools in practice to minimize total vehicle delay (1, 2). There is also a large body of models in the literature following the same general methodology to formulate various delay minimization signal plans, including the works by Stevanovic et al. (3), Yun and Park (4), Liu and Chang (5) and Kashani and Saridis (6). Some more recent studies have also attempted to respond to time-varying traffic dynamics with adaptive controls (7–10).

Widely implemented because of their operational robustness, approaches in the latter category aim to synchronize signals along an arterial with optimized offsets so that vehicles can traverse an arterial segment via the designated progression band. This core concept of progression, first developed by Morgan and Little (11), is to

maximize the green bandwidth so that most vehicles can encounter green phases over consecutive intersections. Their model was further improved by Little (12) with linear programming to optimize concurrently the cycle length, progression speed, and signal offsets.

The enhanced version, called MAXBAND, was introduced by Little et al. (13) to include the impacts because of initial queues and the sequence of left-turn phases. Grounded on the core logic of MAXBAND, Gartner et al. (14) proposed a model, MULTIBAND, where the bandwidths are allowed to vary with traffic volumes on the links. For the same purpose, Chaudhary et al. (15) developed PASSER, a progression optimization program using different formulations. Along the same lines, some researchers have proposed to produce the offsets, based

¹Department of Civil and Environmental Engineering, University of Maryland, College Park, MD

Corresponding Author:

Address correspondence to Yao Cheng: chengyao09@gmail.com

on volumes on different links, with variable phase sequences, or both (16–19). To apply the maximizing progression concept to a long arterial while ensuring the reasonable bandwidth, Tian and Urbanik (20) developed a partition method to divide an arterial into several sub-segments. Note that such a progression design notion has also been refined and applied in developing signal plans for unconventional intersections or traffic networks (21–26).

It should be mentioned that most such studies focus mainly on the efficiency for through movements on an arterial, but not on the performances of left-turn movements albeit the likely presence of considerable left-turn volumes at some of the arterial's major intersections. To accommodate the heavy turning flows and through flows along the arterial, Yang et al. (27) proposed a multi-path progression model which concurrently provides progression bands for several pre-identified vehicle paths with heavy volumes. To ensure the progression for both through and left-turn flows on arterials of heavy volume, however, the following two issues which may degrade the progression quality remain to be tackled by the traffic community. First, in optimizing the offsets for the through progression, not adequately accounting for the left-turn volume and the available bay length at some major intersections may result in rapid queue formation and even spillback over the turning bay, and consequently block some through lanes. Although such spillback and blockage have been extensively studied in the literature (28–31), the anticipated level of progression via the provided bands for the entire arterial may still be inevitably degraded at intersections with short turning bays or heavy left-turn volumes.

Secondly, the potential significant negative impacts from left-turn bay spillback further justify the need to provide progression operations not only for through movements but also for left-turn flows, especially at those arterial intersections serving two crossing major roads and accommodating heavy turning volumes.

In addition, one may note that the delay experienced by left-turn vehicles even under the same progression band may still vary with its relation with where the through band locates within the green phases in the same link. As shown in Figure 1, left-turn vehicles at intersection $k + 1$ within the through bands under Scenario A are sure to experience short or no delays since the through band is located close to the start of the left-turn phase. Under Scenario B, however, with identical bandwidths, most vehicles coming from the upstream intersection k will miss the left-turn phase at intersection $k + 1$ and thus need to wait for the whole red phase. Therefore, the total left-turn delay depends not only on the bandwidth but also on the temporal relation between the left-turn phase and the through band.

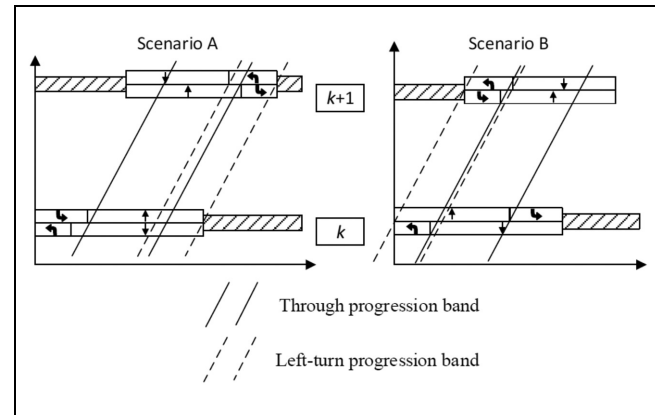


Figure 1. Graphical illustration of different left-turn delays under the same progression bands.

To contend with these two critical issues in the design of an arterial progression plan, this study presents a three-stage optimization model to provide progression to through and left-turn vehicles concurrently via optimized offsets and phase sequences under the bay length constraint. The proposed model also features the capability to: (i) minimize the left-turn delay based on the relation between phase sequences and progression offsets at the subject and its upstream intersections; (ii) identify the duration of queue spillback from the left-turn bay due likely to the heavy turning volume, insufficient bay length, or both; and (iii) mitigate the impacts of such spillback to the through progression band with the optimized offsets and phase sequences.

Model Formulations

Formulation Framework

In response to the aforementioned critical issues, this study proposes a three-stage optimization model, as shown in Figure 2, to optimize the offsets and phase sequences for providing concurrent progression to both through and left-turn flows.

Stage 1 is to obtain the maximum two-way through bandwidths under the optimized offsets and phase sequences with any state-of-the-art model. Note that, because of the adoption of linear programming to model formulations, an effective progression maximization model such as MAXBAND (13) can actually yield multiple optimal sets of offsets for the identical objective value. From these non-inferior solutions, Stage 2 will focus on identifying the ones that can maximize the total effective bandwidth, that is, excluding those progression durations blocked by queue spillback from left-turn flows.

To do so, the proposed model at this stage shall perform the following tasks:

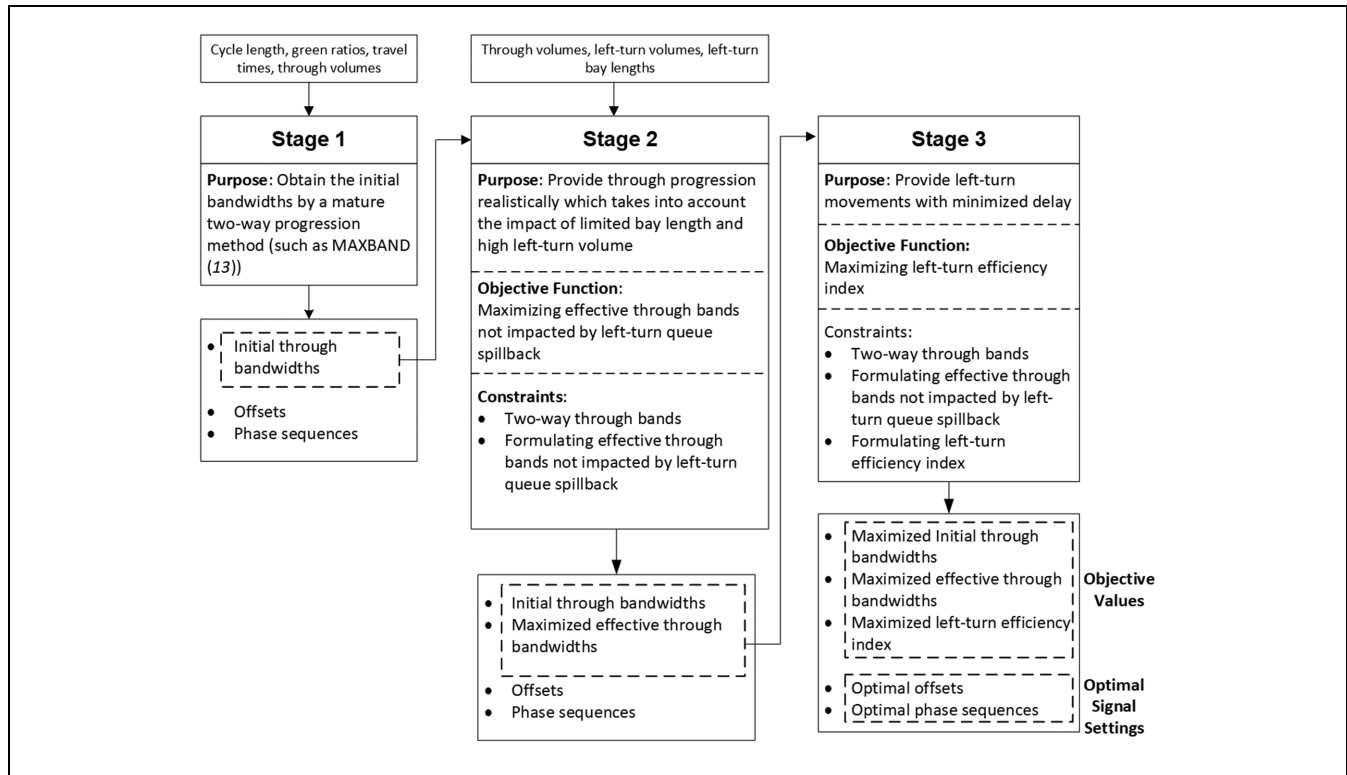


Figure 2. Model framework.

- Estimating when the left-turn queue spillback will occur and vanish, based on the left-turn volume, available bay length, and signal timing plan;
- Analyzing the relations between the left-turn overflow durations at intersections and their impacts on the through bands in each arterial link; and
- Formulating the left-turn queue length based on the temporal relations between the left-turn phase, the through progression band, and the offsets to the upstream intersection.

The estimated maximum effective bandwidth for the through flows under the given left-turn volumes and turning bay length will then serve as the basis to further minimize the delay for left-turn flows with the phase sequences and offsets re-optimized in Stage 3. Figure 2 shows the following three sets of key formulations developed in such a sequential optimization process: (i) calculating the effective bandwidth that can be free from the effect of left-turn queue spillback; (ii) approximating the left-turn delay under given offsets; and (iii) formulating the through progression bands with variable sequences.

Formulating the Impacts of the Left-Turn Queue Spillback on Through Progression Bands

To estimate the portion of the through progression band (i.e., generated without using volume data) blocked by

queue spillback at each major intersection because of either the high left-turn volume or short bay length (see shaded areas in Figure 3a), the starting (e.g., Point A in Figure 3a) and ending times (e.g., Point B in Figure 3a) of the potential queue spillback from the left-turn flows are first estimated.

Starting Time of the Spillback. Given the available left-turn bay length, signal settings, and turning volume, the likely starting time of spillback can be estimated as follows:

$$t_k^O = \frac{k_j n_k^{LT} L_k^{Bay} - Q_k}{q_k^{LT,I}} + \Theta_k^{TH} + w_k \quad (1)$$

$$\bar{t}_k^O = \frac{k_j \bar{n}_k^{LT} \bar{L}_k^{Bay} - \bar{Q}_k}{\bar{q}_k^{LT,I}} + \bar{\Theta}_k^{TH} + \bar{w}_k \quad (2)$$

where k_j , n_k^{LT} (\bar{n}_k^{LT}), and L_k^{Bay} (\bar{L}_k^{Bay}) are the jam density, number of left-turn lanes, and left-turn bay length, respectively; $q_k^{LT,I}$ ($\bar{q}_k^{LT,I}$) denotes the inbound (outbound) flow rates of left-turn vehicles arriving at intersection k within the through progression bands; Q_k (\bar{Q}_k) refers to the number of the vehicles in the left-turn queue when the through band begins; Θ_k^M ($\bar{\Theta}_k^M$) is the start of the green duration for movement M , where $M \in \{LT, TH\}$ (left-turn or through) at intersection k for the inbound (outbound) direction; and w_k (\bar{w}_k) is the gap between the starting times of a green phase and the

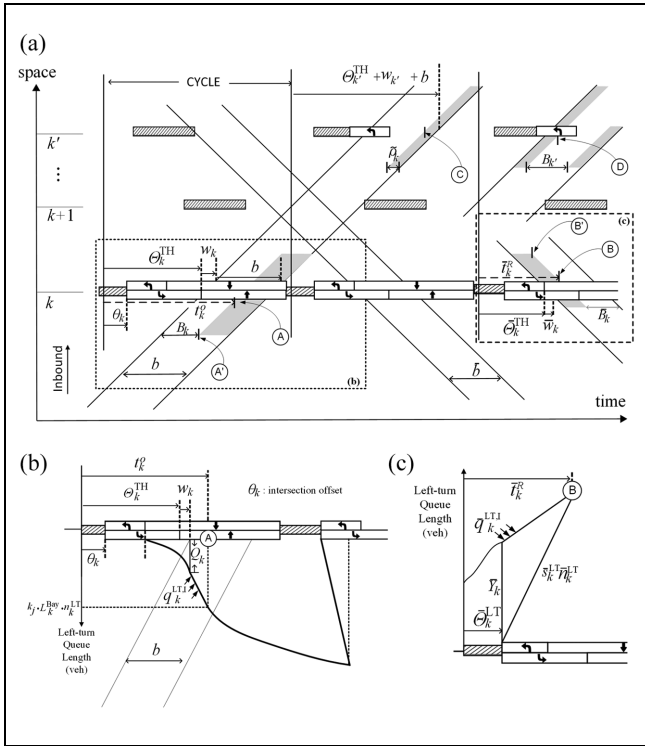


Figure 3. Interrelations between potential queue spillback and reduction of the through bands (a) graphical interruptions of left-turn queue spillback on the through bands; (b) calculating the starting time of left-turn spillback; and (c) calculating the vanishing time of left-turn queues.

progression band for inbound (outbound) direction. The term $k_j n_k^{LT} L_k^{Bay} - Q_k$ is used to calculate the remaining storage space in the left-turn bay at the time when the first vehicle within the through band arrives, as shown in Figure 3b. Note that a large value for t_k^O implies that the likely spillback may take place much later after the start of a green phase for the through movement. If t_k^O is large enough such that the time duration represented by t_k^O actually extends to the end time of the left-turn green in the next signal cycle, then the left-turn queue spillback would not occur.

Vanishing Time of Left-Turning Queues

As shown in Figure 3c, the time for the entire left-turn queue to be discharged can be expressed as follows:

$$t_k^R = \Theta_k^{LT} + \frac{Y_k}{s^{LT} \bar{n}_k^{LT} - \bar{q}_k^{LT, I}} \quad (3)$$

$$\bar{t}_k^R = \bar{\Theta}_k^{LT} + \frac{\bar{Y}_k}{s^{LT} \bar{n}_k^{LT} - \bar{q}_k^{LT, I}} \quad (4)$$

where s^{LT} is the saturation flow rate of left-turn flows and $Y_k(\bar{Y}_k)$ is the number of left-turn vehicles in the queue at

the onset of a left-turn green phase for inbound (outbound) direction. The second term on the right-hand side of Equations 3 and 4 calculates the time duration needed for clearing the queues within the left-turn phase, as demonstrated in Figure 3c with the difference between \bar{t}_k^R and Θ_k^{LT} . When the left-turn queue is cleared, no interruption to the through bands will take place within the same cycle.

Temporal Relation between the Spillback Duration and Through Bands. Although the entire spillback lasts from t_k^O to t_k^R , only part of its duration would interrupt the through band, because the portion not overlapped with the progression band would not have any impact on the vehicles receiving progression. Thus, only the overlapping duration between the left-turn queue spillback and the through band is viewed as the reduced bandwidth. Hence, the effective bandwidth without the interruption by the left-turn queue spillback can be expressed as follows:

$$B_k = b - (\max\{0, \min\{t_k^R, \Theta_k^{TH} + w_k + b\} - \max\{t_k^O, \Theta_k^{TH} + w_k\}\} + \tilde{\rho}_k) \quad (5)$$

$$\bar{B}_k = \bar{b} - (\max\{0, \min\{\bar{t}_k^R, \bar{\Theta}_k^{TH} + \bar{w}_k + \bar{b}\} - \max\{\bar{t}_k^O, \bar{\Theta}_k^{TH} + \bar{w}_k\}\} + \tilde{\rho}_k) \quad (6)$$

where $b(\bar{b})$ denotes the through bandwidth for inbound (outbound) direction; and $\tilde{\rho}_k(\tilde{\rho}_k)$ is an additional term of inbound (outbound) direction, to be addressed later. The terms $\Theta_k^{TH} + w_k$ and $\Theta_k^{TH} + w_k + b$ denote the start and the end of the through band at intersection k , respectively. For example, in Figure 3, the starting time of queue spillback at intersection k for inbound direction (Point A) is within the through band but the queue vanishes at a time point beyond the end of the through band. Thus, the interrupted duration can be expressed as $(\Theta_k^{TH} + w_k + b) - t_k^O$. On the contrary, if the starting time of spillback for the outbound direction is ahead of the through progression band and the vanishing time of the left-turn queue (Point B in Figure 3a) is within the through progression band, the interrupted duration can be denoted by $\bar{t}_k^R - (\bar{\Theta}_k^{TH} + \bar{w}_k)$. Conceivably, if the spillback occurs and is completely cleared before vehicles within the through progression band arrive at the intersection, it would not have any impact on the available bandwidth.

Although each intersection in the entire arterial has its own effective bandwidth, only the minimum of them matters to the arterial since it dictates the potential overall progression efficiency of the through band. Hence, one can define the following constraints for the minimum effective bandwidth for the arterial:

Table 1. Four Types of Scenarios for Computing Left-Turn Queue Length

Condition	Scenario type			
	A	B	C	D
Q_k	$t_k^a \leq t_k^e + N'_k \leq t_k^b + N_{k-1}$	$t_k^b + N_{k-1} \leq t_k^e + N'_k$	$t_k^c + N_{k-1} \leq t_k^e + N'_k \leq t_k^d$	$t_k^d \leq t_k^e + N'_k \leq t_k^c$
Y_k	$q_k^{LT,II} (t_k^b - t_k^e + w_{k-1})$ $q_k^{LT,II} (t_k^c + N_{k-1} - (t_k^e + N'_k) + w_{k-1})$ $- q_k^{LT,I} (\Theta_k^{LT} - t_k^d)$	$q_k^{LT,II} \cdot w_{k-1}$ $q_k^{LT,II} (w_{k-1}) + q_k^{LT,I} (\Theta_k^{LT} - t_k^d)$	$q_k^{LT,II} \cdot [t_k^d - (t_k^e + N'_k)]$ Large number [†]	$q_k^{LT,II} \cdot (\Phi_{k-1}^{TH} - b) + q_k^{LT,I} [t_k^d - (t_k^e + N'_k)]$ $q_k^{LT,II} (\Phi_{k-1}^{TH} - b) + q_k^{LT,I} (b - \Phi_k^{LT})$

[†] Effect of left-turn spillback on the through band does not vanish before end of the through band.

$$B \leq B_k \tag{7}$$

$$\bar{B} \leq \bar{B}_k \tag{8}$$

where $B(\bar{B})$ is the inbound(outbound) effective bandwidth along the arterial. The sum of effective bandwidths for two directions will be maximized in stage 2.

Left-Turn Queue Length. In computing those two critical time points, two key variables are introduced to represent the left-turn queue length at the start of the through band and at the onset of the left-turn phase, denoted by Q_k and Y_k , respectively. These variables are highly related to the offsets between the subject and its upstream intersections, as well as their phase sequences. To facilitate the calculation of these terms, this study has organized all possible scenarios into four types, based on the temporal relations between the following variables (see Table 1):

- The end of the through band, denoted as $t_k^a = \Theta_k^{TH} + w_k + b$
- The time point when the last vehicle from the upstream green phase arrives at the subject intersection, denoted as $t_k^b = \Theta_{k-1}^{TH} + \Phi_{k-1}^{TH} + t_{k-1}$
- The time point when the first vehicle from the upstream green phase arrives at the subject intersection, denoted as $t_k^c = \Theta_{k-1}^{TH} + t_{k-1}$
- The starting time of the through band, denoted as $t_k^d = \Theta_k^{TH} + w_k$
- The end of the left-turn phase, denoted as $t_k^e = \Theta_k^{LT} + \Phi_k^{LT}$

where $\Phi_k^M (\bar{\Phi}_k^M)$ denotes the green split of the movement M ; $t_k(\bar{t}_k)$ is the inbound(outbound) travel time from intersection k to $k + 1(k - 1)$; $q_k^{LT,II} (q_k^{LT,II})$ denotes the inbound(outbound) flow rates of left-turn vehicles arriving at intersection k not within the through progression bands; and N_k and N'_k are integer variables indicating the number of cycles.

For example, if the condition for Type A in Table 1 is satisfied (i.e., $t_k^a \leq t_k^e + N'_k \leq t_k^b + N_{k-1}$), then the left-turn phase shall terminate after the end of the through band and before the last vehicle from the upstream through band arriving at the subject intersection. In this case, the left-turn queue shall start to accumulate after the end of the phase (t_k^e) till t_k^b . Then, after the first vehicle from the upstream through phase arrives at the subject intersection, the queue will continue to increase till the starting time of the through band for a duration of w_{k-1} . Hence, Q_k can be computed by $q_k^{LT,II} (t_k^b - t_k^e + w_{k-1})$, and then its value used to estimate the starting time of the spillback with Equations 1 and 2.

The calculation of the other key variable, Y_k , can also be referred to Table 1. Taking Type B as an example, when $t_k^b + N_{k-1} \leq t_k^e + N'_k \leq t_k^c + N_{k-1}$, vehicles in the left-turn bay will first accumulate at the rate of $q_k^{LT,II}$ over duration w_{k-1} and then the rate will be changed to $q_k^{LT,I}$ from the first vehicle arriving the link via the through band (t_k^d) until the onset of the left-turn green (Θ_k^{LT}). Hence, the queue length at the onset of the left-turn phase can be expressed as $q_k^{LT,II}(w_{k-1}) + q_k^{LT,I}(\Theta_k^{LT} - t_k^d)$. When Y_k is known, one can then estimate the vanishing time of left-turn queue with Equations 3 and 4.

Note that the same notion can be followed to formulate these constraints for the outbound direction.

Impedance by Spillback Impacting Two Consecutive Cycles. If the end of the left-turn phase falls within the time period for the through band (i.e., $t_k^d \leq t_k^e + N'_k \leq t_k^a$), the queue spillback may affect the through bands over two consecutive cycles, that is, from the starting time (Point C) of the left-turn queue spillback to its vanishing time (Point D), as shown in Figure 3a. To facilitate the calculation of interrupted duration for such scenario, an additional term $\tilde{\rho}_k$ has been introduced in Equations 5 and 6 to denote the portion of the interrupted band in the previous cycle, which will apply specifically for Type D in Table 1, as expressed below:

$$\tilde{\rho}_k = \begin{cases} \max\left\{0, t_k^d - \left(\frac{k_{jN}^{LT} L_k^{Bay}}{q_k^{LT,I}} + t_k^e + N'_k\right)\right\} & \text{if type D applies} \\ 0 & \text{o.w.} \end{cases} \quad (9)$$

As shown with Point C in Figure 3a, the duration of impact in the previous cycle ($\tilde{\rho}_k$) begins at the starting time of spillback ($\frac{k_{jN}^{LT} L_k^{Bay}}{q_k^{LT,I}} + t_k^e + N'_k$), and terminates at the end of the through band (t_k^a).

Approximating Left-Turn Delay

Given the offset between two consecutive intersections, the left-turn delay can be approximated based on the temporal relation between the left-turn phase, the through band, and the upstream through phase. To reflect the benefit of left-turn vehicles, this study introduces a left-turn efficiency index which is negatively correlated to the approximated delay. Figure 4 demonstrates the impact of the temporal relation between the left-turn phase, the through band, and the through phase in the upstream intersection on the left-turn efficiency index. For example, if the end of the left-turn phase falls into the time interval between t_k^a and t_k^b (i.e., within interval A), the left-turn vehicles would experience the shortest delay, because the through vehicles from the upstream

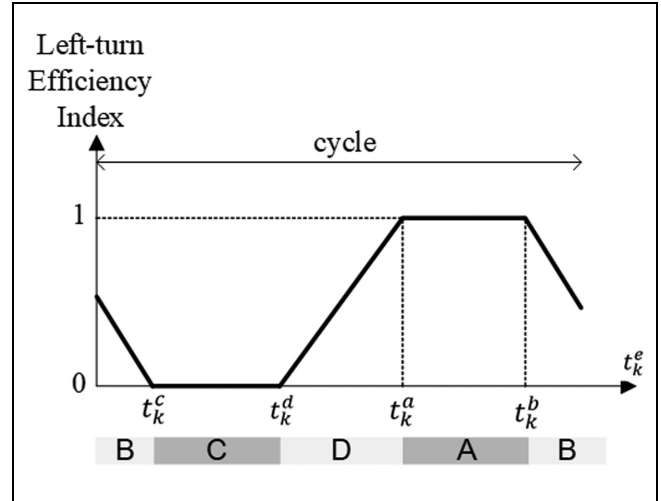


Figure 4. Left-turn efficiency index based on the temporal relations between the end of the left-turn phase, through band, and upstream through phase.

intersection can turn left at the subject intersection with less or no waiting time, resulting in the left-turn efficiency index being 1. In this interval, even left-turn vehicles outside the through band from the upstream intersection may receive the left-turn progression.

On the other extreme, if the left-turn phase terminates within time interval C in Figure 4, all left-turn vehicles within the through band have to stop and wait for the left-turn phase. The left-turn vehicles are expected to experience the longest delay, leading to the lowest left-turn efficiency index. Between these extremes are the intermediate intervals B and D, where the delay is longer when t_k^e is closer to C and is shorter when closer to A. Conditions for defining intervals A to D are the same as those conditions listed in Table 1. In general, the left-turn efficiency index could be expressed as follows:

$$e_k = \begin{cases} 1 & \text{if type A applies} \\ 1 - \frac{(t_k^e + N'_k) - (t_k^c + N_{k-1})}{(1 - \Phi_k^{TH})} & \text{if type B applies} \\ 0 & \text{if type C applies} \\ \frac{(t_k^e + N'_k) - t_k^d}{b} & \text{if type D applies} \end{cases} \quad (10)$$

Through Progression Constraints

To provide through progression, it is necessary to specify the following constraints grounded on the same logic of MAXBAND (13):

$$w_k + b \leq \Phi_k^{TH} \quad (11)$$

$$\bar{w}_k + \bar{b} \leq \bar{\Phi}_k^{TH} \quad (12)$$

$$\Theta_k^{TH} + w_k + N_k + t_k = \Theta_{k+1}^{TH} + w_{k+1} \quad (13)$$

$$\bar{\Theta}_k^{TH} + \bar{w}_k + \bar{N}_k + \bar{t}_k = \bar{\Theta}_{k-1}^{TH} + \bar{w}_{k-1} \quad (14)$$

$$\Theta_k^{TH} = \theta_k + (1 - \chi_k) \cdot (\bar{\Phi}_k^{LT} + I) \quad (15)$$

$$\bar{\Theta}_k^{TH} = \theta_k + (1 - \bar{\chi}_k) \cdot (\Phi_k^{LT} + I) \quad (16)$$

$$\Theta_k^{LT} = \theta_k + (\bar{\chi}_k) \cdot (\bar{\Phi}_k^{TH} + I) \quad (17)$$

$$\bar{\Theta}_k^{LT} = \theta_k + (\chi_k) \cdot (\Phi_k^{TH} + I) \quad (18)$$

$$(1 - K)b \geq (1 - K)K\bar{b} \quad (19)$$

where θ_k represents the intersection offset; K is the ratio of inbound through volume to outbound through volume; $\chi_k(\bar{\chi}_k)$ is a binary variable indicating the phase sequence, which equals 1 if the inbound (outbound) through phase is before the outbound (inbound) left-turn phase; and I represents the intergreen time. The binary variable χ_k allows the model to formulate flexible phase sequences. For example, when $\chi_k = 1$, the inbound through movement will be assigned to the first phase in a cycle; when $\chi_k = 0$, the inbound through phase would be allocated after the outbound left-turn phase. Equation 19 is applied to balance the bandwidths for the two directions.

Objective Functions

The objective function in Stage 2, aiming to maximize the effective two-way bandwidths reflecting the system-wide performance, can be expressed as below:

$$\text{Maximize } B + \bar{B} \quad (20)$$

Note that Stage 2 also requires the bandwidths to be equal to the initial solution from Stage 1, as expressed below:

$$b = b^* \quad (21)$$

$$\bar{b} = \bar{b}^* \quad (22)$$

where $b^*(\bar{b}^*)$ denotes the initial maximized bandwidth for inbound (outbound) traffic obtained in Stage 1.

The objective function in Stage 3 is to maximize the left-turn efficiency index weighted by the number of lanes, which can be expressed as:

$$\text{Maximize } \sum_k n_k^{LT} e_k \quad (23)$$

Similarly, Stage 3 requires the effective bandwidths to be equal to the optimal values in Stage 2:

$$B = B^* \quad (24)$$

$$\bar{B} = \bar{B}^* \quad (25)$$

where $B^*(\bar{B}^*)$ represents the maximum effective bandwidths for inbound (outbound) traffic obtained in Stage 2.

Formulations of Stage 2 and Stage 3

In brief, Stage 2 is formulated as follows,

Maximizing effective bandwidths (Equation 20)
s.t.

- initial through bandwidths (Equations 21 and 22)
- constraints formulating through bands (Equations 11 and 19)
- constraints formulating effective through bands (Equations 1 and 9)

Stage 3 can be formulated as follows,

Maximizing left-turn efficiency (Equation 23)
s.t.

- initial through bandwidths (Equations 21 and 22)
- optimal effective bandwidths (Equations 24 and 25)
- constraints formulating through bands (Equations 11 and 19)
- constraints formulating effective through bands (Equations 1 and 9)
- constraints formulating left-turn efficiency index (Equation 10)

In summary, to smooth the through and left-turn flows along an arterial concurrently under the constraint of the limited left-turn bay length, the proposed model with its three-stage optimization process can effectively address all critical issues raised in the previous section.

Case Study

The purpose of the numerical analysis is to demonstrate that the proposed model can effectively address the following imperative issues:

- Identify the impacts of left-turn spillback and bay length on the arterial progression band, designed mainly for through movements;
- Provide the optimal progression bands and offsets to circumvent or minimize the spillback impacts of left-turn flows on the through movement; and
- Design the phase sequences for critical intersections to maximize the through and left-turn effectiveness under inevitable spillback impacts from heavy left-turn volumes.

To ensure that the effectiveness of the proposed model can be realized in a real-world system, this study has further performed extensive simulation experiments, using the arterial segment of six intersections on MD 193 in Glenn Dale, Maryland. The key parameters associated with the study site are shown in Figure 5.

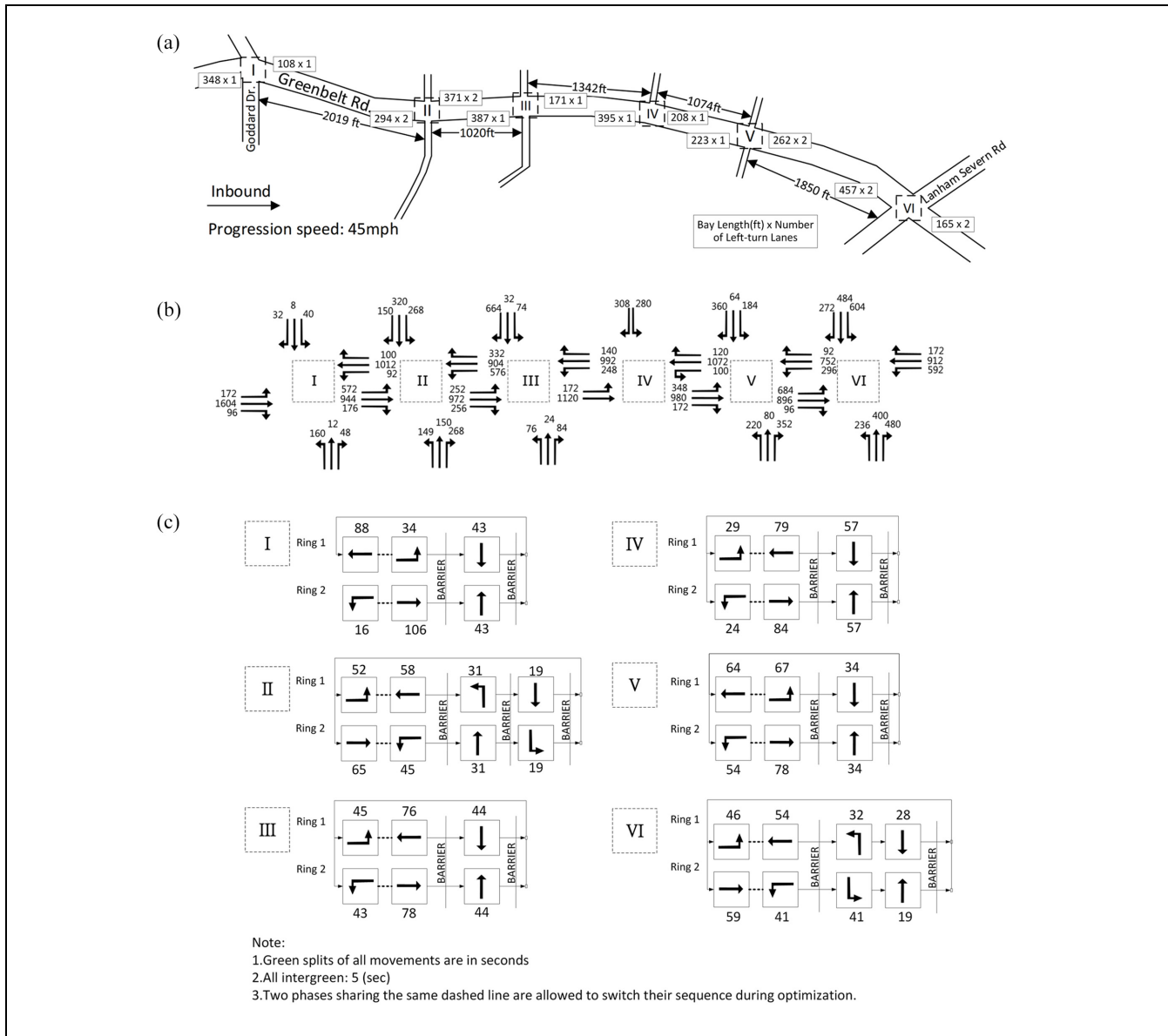


Figure 5. Key information associated with the study site for the case study. (a) Geometric information; (b) traffic volumes; and (c) signal plan.

Numerical Experiments

To explore the effects of left-turn overflows on the through progression bands, the experiment design has adopted a high-demand scenario, as shown in Figure 5b, as the base case. The following three demand levels have also been investigated in the numerical experiments to further assess the interrelations between left-turn volumes and the resulting effective progression bands.

- **Level 1: Low Demand** by reducing the left-turn volumes by 200 vph at intersections II, V, and VI, but increasing the through volumes by 100 vph.

- **Level 2: Medium Demand** by reducing the left-turn volumes by 80 vph at intersection II, V, and VI, but increasing the through volumes by 40 vph.
- **Level 3: Heavy-Turning Demand** by increasing 80 vph of the left-turn volumes, but reducing 40 vph of the through flows at intersection II, V, and VI.

Table 2 shows the initial bandwidth, left-turn efficiency index, and the effective bandwidths produced by the proposed model and one of the most effective state-of-the-art models, MAXBAND, which does not consider the spillback of left-turn volume and the bay length constraints in the offset and phase sequence optimization.

Table 2. Comparison of the Progression Bandwidths and Left-Turn Efficiency Indices under Different Volume Levels

Phase sequence	Demand scenario	Initial bandwidth ^a (sec)		Effective bandwidth not impeded by spillback (sec)				Average left-turn efficiency index
		Inbound	Outbound	By MAXBAND		By the proposed model		
Fixed	Level 1 (low)	49.6	43.3	49.6	43.3	49.6	43.3	0.568
	Level 2 (medium)	49.5	43.6	(0)	(0)	(0)	(0)	0.560
	Base case (high)	49.6	42.9	30.2 (39.0%)	43.6 (0)	49.5 (0)	43.6 (0)	0.545
	Level 3 (high turning volume)	49.7	42.9	6.7 (86.5%)	42.9 (0)	37.5 (24.4%)	42.9 (0)	0.545
Variable	Base case (high)	49.9	43.3	0 (100.0%)	42.9 (0)	26.7 (46.3%)	42.9 (0)	0.619
	Level 3 (high turning volume)	50.0	43.2	9.6 (80.8%)	31.2 (27.9%)	49.9 (0)	43.3 (0)	0.617

^aInitial bandwidths with MAXBAND, but neglecting the impacts of overflows from the left-turn volume. The numbers in parenthesis indicate the reduced percentage of bandwidth.

Minimizing the Impact of Left-Turn Bay Spillback on the Through Progression Bands. As shown in Table 2, when the left-turn volume is relative low, spillback from the left-turn queue may not take place and will certainly not interrupt the through bands. When the left-turn volume is at the medium level, about 39.0% of inbound progression bandwidth generated by MAXBAND will be impeded by the queue spillback from the overflows, but not with our proposed model. The results are also evident that the proposed model can capture the impacts resulting from left-turn queue spillback and estimate the effective bandwidth for the inbound flows to be 49.5 seconds, compared with 30.2 seconds generated by MAXBAND.

In the base scenario of high demand, the proposed model under the fixed-phase sequence design, despite its minimization of queue spillback impacts (i.e., reducing from 86.5% to 24.4%), continues to suffer from heavy turning flows and insufficient bay length. By concurrently optimizing the signal phase sequence in the progress of progression bandwidth maximization, the proposed model, however, can achieve the best left-turn progression, thereby eliminating their interference to the through progression flows (i.e., from 24.4% to 0%).

Conceivably, under very heavy left-turn volume and insufficient bay length, the progression bands produced by MAXBAND may not practically exist, considering their portions being blocked by the spillback flows (see level 3) even with the optimized phase sequences. The proposed model, however, can minimize such impacts and keep a substantial percentage of the through band intact, that is, from no progression band to a 46.3% reduction.

The Effectiveness of Left-Turn Progression. The resulting left-turn efficiency indices (see Equation 10) under different demand levels are also shown in Table 2. Notably, by properly taking into account the relationship between left-turn volume and through flows in generating offsets, the proposed model can ensure a relatively stable progression for left-turn flows (i.e., left-turn efficiency indices between 0.568 and 0.545). Left-turn progression can be improved significantly if the phase sequence is also allowed to be a decision variable because the flexibility of the phase sequences allows the signal plan to accommodate better the interactions between the left-turn flows and traffic from its upstream through phase.

In conclusion, the above results clearly demonstrate the benefits and needs of including through and left-turning volumes as well as bay length in design of the signal progression plan for an arterial generally experiencing heavy left-turn volumes at some of its major intersections. By allowing the phase sequences to vary with the turning volume and the interactions between through flows and spillback flows, the proposed model indeed offers the potential to produce the optimized offsets and progression bands which can actually be experienced by arterial users (see Table 2).

Simulation Evaluation

To ensure that the arterial under the control objective of maximizing the progression produced by the proposed model will not be at the expense of other measures of effectiveness (MOEs) (e.g., delay, number of stops), this study has further conducted simulation experiments with

Table 3. Signal Plans Generated by the Proposed Model and MULTIBAND

Intersection	Proposed model			MULTIBAND		
	Offset ^a	Phase sequence		Offset	Phase sequence	
		Ring 1 ^b	Ring 2 ^c		Ring 1 ^b	Ring 2 ^c
I	0	0	0	0	0	0
II	92	1	1	92	1	1
III	66	1	0	65	1	0
IV	96	0	0	103	0	0
V	87	0	0	89	0	0
VI	8	1	1	10	1	1

^aOffsets are references to intersection I.

^bRing 1 is composed of outbound TH and inbound LT, see Figure 5. If the value is one, outbound TH precedes inbound LT; otherwise, the LT phase precedes TH phase.

^cRing 2 is composed of inbound TH and outbound LT, see Figure 5. If the value is one, inbound TH precedes outbound LT; otherwise, the LT phase precedes TH phase.

Table 4. MOEs Produced from the Simulation Experiments

Direction	Signal	MULTIBAND		Proposed model		Percentage change	
		Average delay (sec/veh)	Average # of stops (-/veh)	Average delay (sec/veh)	Average # of stops (-/veh)	Average delay	Average # of stops
Overall arterial performance for through movements							
Overall	na	110.1	2.35	103.1 s	2.22	-6.4%	-5.5%
Inbound	na	83.4	2.36	82.0 s	2.38	-1.7 %	0.84%
Outbound	na	139.7	2.35	125.8 s	2.04	-9.9 %	-13.2 %
Performance of through movements at the selected intersections							
Outbound	IV	17.9	0.45	15.7	0.38	-12.2%	-17.0%
	III	35.9	0.74	30.9	0.63	-14.0%	-14.0%
	II	38.2	0.65	37.8	0.66	-1.1%	1.4%
Performance of left-turn movements with high left-turn efficiency indices							
Inbound	IV	92.7	2.65	86.0	2.63	-7.2%	-0.75%
	V	72.6	2.16	72.1	2.19	-0.70%	1.3%
Outbound	II	140.5	2.40	126.3	2.15	-10.1%	-10.4%
	V	85.6	1.18	84.3	1.15	-1.4%	-2.2%

Note: MOEs = measures of effectiveness; na = not applicable.

VISSIM under the base scenario. The generated signal plan is shown in Table 3; the simulation results and comparison with MULTIBAND are shown in Table 4 and Figure 6. Notably, the signal progression plan produced by the proposed model, as expected, can produce not only the maximum effective bandwidth, but also shortest average delay and least number of stops to both the through and left-turn vehicles.

As seen in the first data set of Table 4, the proposed model is able to reduce the delay and number of stops by 6.4% and 5.5%, respectively, for through movements on the entire arterial segment. This is because of the capability of the developed model to reduce the interruptions

from the left-turn queues to the through band. For example, the outbound through movement at intersection IV shows a 12.2% reduction on the average delay and a 17.0% reduction on the number of stops.

To further demonstrate the effectiveness of the proposed model, Figure 6 shows the median value of left-turn vehicle queues within the through bands for the outbound direction at intersection III. The horizontal dashed line shows the length of the left-turn bay and the bars denote median values of the maximum queue length in each cycle. Note that the queue under the control with the proposed model is obviously shorter than that under MULTIBAND and does not cause spillbacks in most

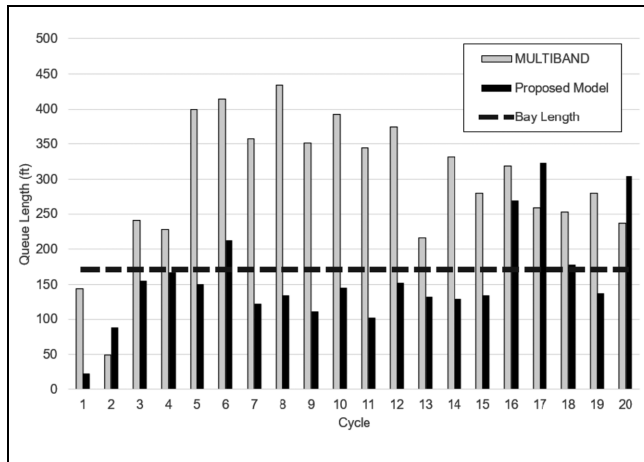


Figure 6. Median of maximum left-turn queue lengths within the through progression bands at intersection III for the outbound direction.

cycles. Among all 200 signal cycles from 10 simulation replications, just 38.5% experienced left-turn spillback under the proposed model, significantly lower than the resulting 80.5% under the same scenarios with MULTIBAND.

Note that left-turn flows also enjoy a shorter delay and lower number of stops since the proposed model can maximize the left-turn efficiency index, as shown in Table 4. For example, at intersection IV, the inbound direction has a left-turn efficiency index of one under the proposed model, contributing to a 7.2% reduction of the average delay for the left-turn vehicles.

In brief, the results of the extensive experiments indicate that the proposed model can successfully generate the maximized effective bandwidth (not interrupted by the left-turn spillback queues) by taking into account the left-turn volume and bay length, as evidenced by the reduced delay and number of stops for the through movement on the arterial with heavy left-turn flows. The left-turn traffic condition has also been improved since their progressions are concurrently designed in the proposed model.

Conclusions

To contend with spillback blockages often observed between left-turn queues and through flows on major arterials whose signal plans are designed mainly to facilitate through traffic movements, this study has presented a three-stage optimization model to offer progression for both the through and left-turning flows. The proposed model features the capability first to compute the percentage of through progression band likely to be blocked by the queues overflowing from the left-turn bay. Depending on the initial two-way through bandwidths obtained in Stage 1, one can then proceed to Stage 2 of

the proposed model to compute the optimal offsets that can maximize the effective bandwidths not affected by such spillback under the given left-turn volumes and bay lengths. Since the arriving pattern of the left-turn flows and its queue formation pace vary with the signal phasing and timings at the upstream intersection, Stage 3 of the proposed model further offers the function to search the offsets and phase sequences which can also yield the minimum delay for the left-turn flows without compromising the total effective bandwidth for the entire arterial.

The results of the extensive evaluation with both numerical analyses and simulation experiments have confirmed the effectiveness of the proposed model in producing the through and left-turn progression bands that may not effectively exist under some traffic scenarios, if with conventional arterial progression models, because of the spillover blockage from turning bays. For example, under the base demand level shown in the experimental analysis, the interruption to the inbound through band because of left-turn queue spillback has been reduced from 80.8%, if produced by MAXBAND, to 0.0% with the proposed model. Further evaluation with simulation experiments also provides assurance that the produced optimal offsets and phase sequences for maximizing the through and left-turn progression bands will not be at the cost of other MOEs. For instance, the signal plan generated by the proposed model can decrease the average delay by 6.4% and the number of stops by 5.5% in the base case scenario for the through movements along the arterial, compared with MULTIBAND, the state-of-the-art model.

Hence, this proposed model has the potential to be used in practice, especially for urban arterials consisting of some major intersections plagued by high turning volumes and limited bay lengths.

One of the ongoing extensions along this line is to include the potential blockage to the left-turn flows by the through queues at critical intersections and the issue of shared left-turn lanes. A detailed analysis of the capacity of through and left-turn lanes under left-turn spillback conditions should also be integrated into the design of progression plans. A probabilistic model to estimate the occurrence of the queues can also further improve the robustness of the progression design in response to the time-varying traffic flows.

Author Contributions

The authors confirm contribution to the paper as follows: study conception and design: Y-HC, YC, G-LC; data collection: Y-HC; analysis and interpretation of results: Y-HC, YC; draft manuscript preparation: YC, Y-HC, G-LC. All authors reviewed the results and approved the final version of the manuscript.

References

1. Robertson, D. I. *TRANSYT: A Traffic Network Study Tool*. TRRL Report LR 253. Road Research Laboratory, U.K., Crowthorne, Berkshire, 1969.
2. Wallace, C. E., K. G. Courage, D. P. Reaves, G. W. Shoene, G. W. Euler, and A. Wilbur. *TRANSYT-7F User's Manual: Technical Report*. University of Florida, Gainesville, FL, 1988.
3. Stevanovic, A., P. T. Martin, and J. Stevanovic. VisSim-Based Genetic Algorithm Optimization of Signal Timings. *Transportation Research Record: Journal of the Transportation Research Board*, 2007. 2035: 59–68.
4. Yun, L., and B. Park. Application of Stochastic Optimization Method for an Urban Corridor. *Proc., Winter Simulation Conference*, 2006, Monterey, CA, pp. 1493–1499.
5. Liu, Y., and G. L. Chang. An Arterial Signal Optimization Model for Intersections Experiencing Queue Spillback and Lane Blockage. *Transportation Research Part C: Emerging Technologies*, Vol. 19, No. 1, 2011, pp. 130–144.
6. Kashani, H. R., and G. N. Saridis. Intelligent Control for Urban Traffic Systems. *Automatica*, Vol. 19, 1983, pp. 191–197.
7. Christofa, E., K. Ampountolas, and A. Skabardonis. Arterial Traffic Signal Optimization: A Person-Based Approach. *Transportation Research Part C: Emerging Technologies*, Vol. 66, 2016, pp. 27–47.
8. Keyvan-Ekbatani, M., A. Kouvelas, I. Papamichail, and M. Papageorgiou. Exploiting the Fundamental Diagram of Urban Networks for Feedback-Based Gating. *Transportation Research Part B: Methodological*, Vol. 46, No. 10, 2012, pp. 1393–1403.
9. Aboudolas, K., and N. Geroliminis. Perimeter and Boundary Flow Control in Multi-Reservoir Heterogeneous Networks. *Transportation Research Part B: Methodological*, Vol. 55, 2013, pp. 265–281.
10. Keyvan-Ekbatani, M., M. Papageorgiou, and I. Papamichail. Urban Congestion Gating Control Based on Reduced Operational Network Fundamental Diagrams. *Transportation Research Part C: Emerging Technologies*, Vol. 33, 2013, pp. 74–87.
11. Morgan, J. T., and J. D. C. Little. Synchronizing Traffic Signals for Maximal Bandwidth. *Operation Research*, Vol. 12, No. 6, 1964, pp. 896–912.
12. Little, J. D. C. The Synchronization of Traffic Signals by Mixed-Integer Linear Programming. *Operation Research*, Vol. 14, No. 4, 1966, pp. 568–594.
13. Little, J. D., M. D. Kelson, and N. M. Gartner. MAX-BAND: A Program for Setting Signals on Arteries and Triangular Networks. *Transportation Research Record: Journal of the Transportation Research Board*, 1981. 795: 40–46.
14. Gartner, N. H., S. F. Assman, F. Lasaga, and D. L. Hou. A Multi-Band Approach to Arterial Traffic Signal Optimization. *Transportation Research Part B*, Vol. 25, No. 1, 1991, pp. 55–74.
15. Chaudhary, N. A., V. G. Kovvali, C.-L. Chu, J. Kim, and S. M. Alam. *Software for Timing Signalized Arterials*. Report FHWA/TX-03/4020-1. Texas Transportation Institute, the Texas A&M University System, College Station, Texas, 2002.
16. Zhang, C., Y. Xie, N. H. Gartner, C. Stamatiadis, and T. Arsava. AM-Band: An Asymmetrical Multi-Band Model for Arterial Traffic Signal Coordination. *Transportation Research Part C: Emerging Technologies*, Vol. 58, 2015, pp. 515–531.
17. Papola, N. Bandwidth Maximization: Split and Unsplit Solutions. *Transportation Research Part B: Methodological*, Vol. 26, No. 5, 1992, pp. 341–356.
18. Messer, C. J., R. H. Whitson, C. L. Dudek, and E. J. Romano. A Variable-Sequence Multiphase Progression Optimization Program. *Highway Research Record*, No. 445, 197, pp. 24–33.
19. Li, J. Q. Bandwidth Synchronization under Progression Time Uncertainty. *IEEE Transactions on Intelligent Transportation Systems*, Vol. 15, No. 2, 2014, pp. 1–11.
20. Tian, Z., and T. Urbanik. System Partition Technique to Improve Signal Coordination and Traffic Progression. *Journal of Transportation Engineering*, Vol. 133, No. 2, 2007, pp. 119–128.
21. Yang, X., G. L. Chang, and S. Rahwanji. Development of a Signal Optimization Model for Diverging Diamond Interchange. *Journal of Transportation Engineering*, Vol. 140, No. 5, 2014, p.04014010.
22. Cheng, Y., G. L. Chang, and S. Rahwanji. Concurrent Optimization of Signal Progression and Crossover Spacing for Diverging Diamond Interchanges. *Journal of Transportation Engineering, Part A: Systems*, Vol. 144, No. 3, 2018, p. 04018001.
23. Yang, X., Y. Cheng, and G.L. Chang. Operational Analysis and Signal Design for Asymmetric Two-Leg Continuous-Flow Intersection. *Transportation Research Record: Journal of the Transportation Research Board*, 2016. 2553: 72–81.
24. Chang, E. C., S. L. Cohen, C. Liu, N. A. Chaudhary, C. and Messer, C. MAXBAND-86: Program for Optimizing Left-Turn Phase Sequence in Multiarterial Closed Networks. *Transportation Research Record: Journal of the Transportation Research Board*, 1988. 1181: 40–46.
25. Gartner, N. H., and C. Stamatiadis. Arterial-Based Control of Traffic Flow in Urban Grid Networks. *Mathematical and Computer Modelling*, Vol. 35, No. 5–6, 2002, pp. 657–671.
26. Gartner, N. H., and C. Stamatiadis. Progression Optimization Featuring Arterial-and Route-Based Priority Signal Networks. *Journal of Intelligent Transportation Systems*, Vol. 8, No. 2, 2004, pp. 77–86.
27. Yang, X., Y. Cheng, and G. L. Chang. A Multi-Path Progression Model for Synchronization of Arterial Traffic Signals. *Transportation Research Part C: Emerging Technologies*, Vol. 53, 2015, pp. 93–111.
28. Tian, Z. Z., and N. Wu. Probabilistic Model for Signalized Intersection Capacity with a Short Right-Turn Lane. *Journal of Transportation Engineering*, Vol. 132, No. 3, 2006, pp. 205–212.
29. Zhang, Y., and J. Tong. Modeling Left-Turn Blockage and Capacity at Signalized Intersection with Short Left-Turn

- Bay. *Transportation Research Record: Journal of the Transportation Research Board*, 2008. 2071: 71–76.
30. Osei-Asamoah, A., A. Kulshrestha, S. S. Washburn, and Y. Yin. Impact of Left-Turn Spillover on Through Movement Discharge at Signalized Intersections. *Transportation Research Record: Journal of the Transportation Research Board*, 2010. 2173: 80–88.
31. Reynolds, W., N. Rouphail, and X. Zhou. Turn Pocket Blockage and Spillback Models: Applications for Signal Timing and Capacity Analysis. *Transportation Research Record: Journal of the Transportation Research Board*, 2011. 2259: 112–122.
- The Standing Committee on Traffic Signal Systems (AHB25) peer-reviewed this paper (19-05184).*